Achieving Optimal Quantum Acceleration of Frequency Estimation Using Adaptive Coherent Control

M. Naghiloo,[1] A. N. Jordan,[2,3,4] and K. W. Murch[1,5,*]

[1]Department of Physics, Washington University, St. Louis, Missouri 63130, USA
[2]Department of Physics and Astronomy, University of Rochester, Rochester, New York 14627, USA
[3]Center for Coherence and Quantum Optics, University of Rochester, Rochester, New York 14627, USA
[4]Institute for Quantum Studies, Chapman University, Orange, California 92866, USA
[5]Institute for Materials Science and Engineering, St. Louis, Missouri 63130, USA

(Received 18 June 2017; published 1 November 2017)

Precision measurements of frequency are critical to accurate time keeping and are fundamentally limited by quantum measurement uncertainties. While for time-independent quantum Hamiltonians the uncertainty of any parameter scales at best as $1/T$, where T is the duration of the experiment, recent theoretical works have predicted that explicitly time-dependent Hamiltonians can yield a $1/T^2$ scaling of the uncertainty for an oscillation frequency. This quantum acceleration in precision requires coherent control, which is generally adaptive. We experimentally realize this quantum improvement in frequency sensitivity with superconducting circuits, using a single transmon qubit. With optimal control pulses, the theoretically ideal frequency precision scaling is reached for times shorter than the decoherence time. This result demonstrates a fundamental quantum advantage for frequency estimation.

DOI: 10.1103/PhysRevLett.119.180801

The ability to sense more accurately has historically been the basis of many of our scientific advances and technological innovations. In particular, precision measurements have been instrumental in advancing our knowledge of fundamental physical laws [1–4]. Notably, frequency measurements have been essential to experimental tests of general relativity, the standard model of particle physics, and quantum mechanics and are the practical foundation of all time keeping devices. The precision of measurements is ultimately governed by the fundamentally probabilistic nature of quantum measurements, which arises most basically in the Heisenberg uncertainty principle. Traditionally, frequency measurements, such as are conducted with atomic clocks [5–7], are associated with the measurement of the energy difference E between two eigenvalues of a static Hamiltonian H, and the frequency uncertainty arises from the energy-time uncertainty principle [8] $\delta\omega = \delta E/\hbar = 1/(2T)$, where T is the time of the experiment. New situations arise in frequency metrology when one considers instead *time-dependent* Hamiltonians, where the precision of frequency measurements can be optimized with additional control.

In metrology, one seeks to determine a parameter g from repeated measurements that naturally follow a probability distribution $p_g(X)$, where X is some random variable. For large data sets, the Cramér-Rao bound [9] gives a universal limit for the mean squared deviation of the parameter:

$$\langle \delta^2 \hat{g} \rangle \geq \frac{1}{v I_g}, \tag{1}$$

where v is a measure of the amount of data, $\hat{g}$ is an unbiased estimator of the parameter g formed from measurement data, and $I_g = \int p_g(X)[\partial_g \ln p_g(X)]^2 dX$ is the Fisher information [10], which characterizes the amount of information about the parameter g that is contained in the data. Therefore, the Fisher information is a natural measure of how optimal a given measurement strategy is for determining the parameter g with minimal uncertainty.

For quantum parameter estimation, measurements on quantum states $|\psi_g\rangle$ are used to find the probability distribution $p_g(X)$. In this case, the Fisher information in the quantum state is given by [11,12]

$$I_g^{(Q)} = 4(\langle \partial_g \psi_g | \partial_g \psi_g \rangle - |\langle \psi_g | \partial_g \psi_g \rangle|^2), \tag{2}$$

which maximizes the classical Fisher information in the measurement results on the state over all possible types of quantum measurements. The quantum Fisher information is a measure of the distinguishability of two states $|\psi_g\rangle$ and $|\psi_{g+dg}\rangle$, and with this formulation, it is clear that some quantum states garner more quantum Fisher information than others. In particular, nonclassical correlations can enhance measurement sensitivities. The use of such nonclassical resources in measurement has been widely studied [13–15] and applied in several metrological areas including imaging [16], gravitational waves [17], and magnetometry [18]. Much of this research has focused on the scaling of the quantum Fisher information with the number N of quantum systems; whereas uncorrelated systems lead to the standard quantum limit $\propto N$, appropriate quantum correlations can lead to the Heisenberg scaling $\propto N^2$ [15].

Here, we focus rather on how the quantum Fisher information for a single quantum system scales with time [19].

If, for example, the parameter to be estimated is a multiplicative factor [20] on a static Hamiltonian, $H_g = gH_0$, then, given that unitary evolution for a time T is described by $U_g = \exp(-igH_0T)$, the quantum Fisher information scales in time as $I_g \propto T^2$ [20]. However, if the Hamiltonian is instead time dependent [14,21], the quantum Fisher information may exceed this scaling for certain parameters, reaching a scaling of $I_g \propto T^4$ for estimating the frequency of an oscillating Hamiltonian under optimal coherent control [22]. Very recent experiments [23–25] in magnetic-field-sensing NV centers have demonstrated that using a hybrid quantum-classical strategy of estimating a local magnetic field value with a quantum technique, repeated in time, together with a classical Fourier transform can achieve a Fisher information of the frequency scaling as T^3. In this Letter, we experimentally demonstrate T^4 scaling of the quantum Fisher information in the estimation of a Hamiltonian oscillation frequency for a pseudo-spin-half system. This quantum enhanced scaling has been proved [22] to be the best allowed by quantum mechanics in the kind of system we consider in this work. This improved scaling is achieved through adaptive optimal control where an additional control Hamiltonian that depends on the estimated parameter is applied to the system to enhance sensitivity. We show that the T^4 scaling is robust against small variations in the control Hamiltonian, thus allowing for adaptive control.

To illustrate how optimal control can be used to maximize the quantum Fisher information, we consider a time-dependent Hamiltonian imposed on a two-level quantum system $H_\omega(t) = A\hbar\sin(\omega t)\sigma_z/2$, describing the periodic modulation of the energy levels of the system with amplitude A as shown in Fig. 1(a). Our focus is to maximize the quantum Fisher information of the modulation frequency ω, that is, to minimize the overlap of two quantum states $|\psi_\omega\rangle$ and $|\psi_{\omega+\delta\omega}\rangle$ after time evolution under the Hamiltonian for time T. We will show that the optimal choice of quantum states is a superposition of energy eigenstates $(|0\rangle + e^{i\phi}|1\rangle)/\sqrt{2}$, which accumulate different phases $\phi_\omega(T)$ under the Hamiltonian evolution.

To formalize our discussion of the quantum Fisher information, we reformulate Eq. (2) as $I_\omega^{(Q)} = 4\mathrm{Var}[h_\omega(T)]_{|\psi_0\rangle}$, where $h_\omega(T) = iU_\omega^\dagger(0\to T)\partial_\omega U_\omega(0\to T)$, $U_\omega(0\to T)$ is the unitary evolution of the initial state $|\psi_0\rangle$ under the Hamiltonian, and $\mathrm{Var}[\cdot]$ represents the variance. In this form, we can see that the quantum Fisher information is related to the squared difference between the minimum and maximum eigenvalues of $h_\omega(T)$.

To determine the eigenvalues of $h_\omega(T)$, we break the unitary evolution $U_\omega(0\to T)$ into infinitesimal time intervals as discussed in Ref. [22] and consider the eigenvalues of $h_\omega(t)$ versus the time. In the current case, the Hamiltonian commutes with itself at different times, so we arrange the system to be in a superposition of the eigenstates of $\partial_\omega H_\omega(t)/\hbar$, such that the eigenvalues maintain maximal separation. These eigenvalues simply evolve as $\mu_\pm(t) = \pm At\cos(\omega t)/2$. In Fig. 1(b), we sketch $\mu_\pm(t)$. The quantum Fisher information (QFI) about the frequency ω associated with an evolution for time T is given by

$$I_\omega^{(Q)} = \left(\int_0^T [\mu_+(t) - \mu_-(t)]dt\right)^2, \qquad (3)$$

which increases as T^2. Figure 1(c) displays how additional control at the crossing points can be used to dramatically enhance the QFI. By applying a control to guide the qubit along a trajectory that maximizes the integral (3), the QFI can increase instead as T^4 as shown in Fig. 1(d). The intuitive reason for the T^4 scaling versus the T^2 scaling is that, for time-independent Hamiltonians, two nearby quantum states corresponding to different values of the parameter can only diverge from each other with constant velocity, whereas in time-dependent Hamiltonians, they can accelerate away from each other, giving greater quantum distinguishability of the states in the same period of time [22,26,27].

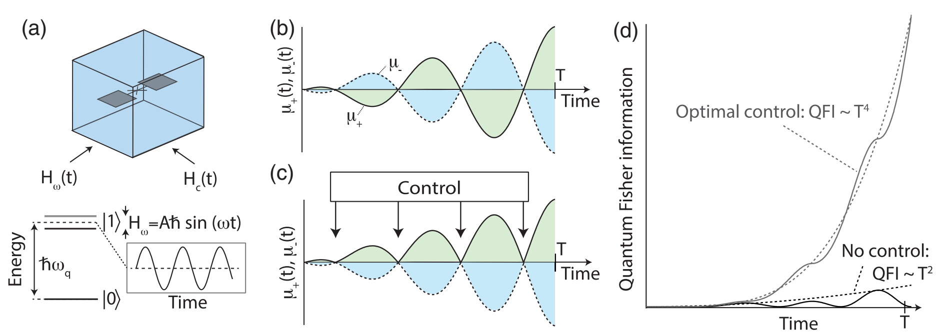

FIG. 1. Frequency estimation of a time-periodic Hamiltonian. (a) The experiment consists of a transmon qubit dispersively coupled to a waveguide cavity. The qubit is subject to a time-dependent Hamiltonian $H_\omega(t)$, and the task is to estimate the frequency ω. (b) The eigenvalues $\mu_\pm$ of $\partial_\omega H_\omega(t)/\hbar$. The quantum Fisher information is related to the integral of $\mu_+(t) - \mu_-(t)$, which is alternately positive or negative. (c) A control $H_c(t)$ is used to guide the qubit evolution such that $\mu_+(t)$ and $\mu_-(t)$ are maximally separated. (d) The scaling of the quantum Fisher information for the uncontrolled and controlled measurement evolution, showing scaling as T^2 and T^4, respectively.

We now turn to the experiment, where we realize the optimal control depicted in Fig. 1(c). The experimental setup consists of a superconducting transmon circuit [28] that is dispersively coupled to a waveguide cavity [29]. The qubit system is comprised of the lowest two levels of the circuit and is described by the Pauli spin operators σ_x, σ_y, and σ_z. The dispersive interaction between the qubit and the cavity, described by the Hamiltonian $H_{\rm int} = -\hbar\chi\hat{n}\sigma_z$, allows for the rapid, quantum nondemolition measurement of the qubit in the energy basis by probing the cavity resonance with microwave photons. Here $\chi/2\pi = -0.5$ MHz is the dispersive coupling rate, and $\hat{n}$ is the cavity photon number operator. To create the time-dependent Hamiltonian $H_\omega = A\hbar\sin(\omega t)\sigma_z/2$, we drive the cavity with detuning $\Delta/2\pi = 37$ MHz to populate the cavity with an average $\bar{n} = \bar{n}_0 + A\sin(\omega t)/2\chi$ photons. The mean photon number $\bar{n}_0 = 6.4$ results in an ac Stark shift of 6.4 MHz and the modulation amplitude $A/2\pi = 0.60$ MHz.

We first demonstrate the standard T^2 scaling of the quantum Fisher information that is obtained without Hamiltonian control. An equal superposition state $(|0\rangle + e^{i\phi}|1\rangle)/\sqrt{2}$ maximizes the QFI, and the measurement protocol is simply a Ramsey sequence as depicted in Fig. 2(a). A $\pi/2$ pulse is applied, followed by waiting for a time T, followed by a second $\pi/2$ pulse and projective measurement in the σ_z basis. The axis of the second $\pi/2$ rotation is adjusted such that the projective measurement in the energy basis accumulates maximal information about the phase of the qubit. The QFI is given in terms of the Bures distance [30] $ds^2 = 2(1 - |\langle\psi_\omega|\psi_{\omega+d\omega}\rangle|)$, where $I_\omega^{(Q)} = 4ds^2/d\omega^2$. As such, we vary ω by a small amount to determine the slope [Fig. 2(c)], where $I_\omega^{(Q)} = (d\phi/d\omega)^2$. The frequency sensitivity is ultimately governed by the QFI and the phase variance, which as shown in Fig. 2(d) is given by the standard binomial error $\delta\phi = 1/\sqrt{4N}$ due to projection noise, resulting in a cumulative frequency information of $NI_\omega^{(Q)}$. As displayed in Fig. 2(e), the frequency sensitivity improves as $\omega/(AT)$, (QFI $\propto T^2$) until dephasing of the qubit, characterized by $T_2^* = 4$ μs, degrades the sensitivity.

The key idea behind optimal coherent control is to impose an additional time-dependent Hamiltonian $H_c(t)$ to maximize the difference of the eigenvalues of $h_\omega(T)$. In Fig. 2(b), we display this optimal Hamiltonian control, which consists of discrete unitary π rotations applied to the qubit at specific optimal times: These are applied at the *antinodes* of the estimated Hamiltonian rather than at the nodes as is commonly seen in dynamical decoupling sequences [26]. In contrast to dynamical decoupling pulses, whose object is to refocus diverging states and prolong coherence, our control pulses do the opposite: The objective is to separate as quickly as possible two quantum states corresponding to nearby values of the frequency in order to improve our resolution of that parameter; hybrid schemes have very recently been proposed [27]. In Fig. 2(e), we show how under optimal control the frequency sensitivity attains the ultimate limit $\delta\omega/\delta\phi = \pi/(AT^2)$ for short times

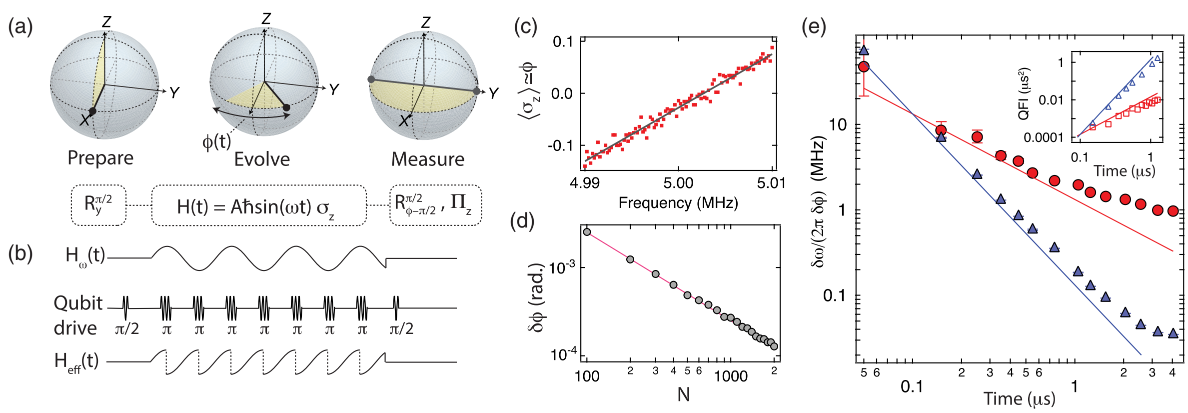

FIG. 2. Frequency metrology with optimal control. (a) Schematic of the estimation task: The qubit is prepared in a superposition of energy eigenstates $(|0\rangle + |1\rangle)/\sqrt{2}$, followed by an interaction with a time-periodic Hamiltonian with frequency ω for a certain time, followed by a $\pi/2$ pulse and projection in the σ_z basis to determine the acquired phase. (b) The energy eigenvalue difference of Hamiltonian $H_\omega(t)$ is sketched in time, together with the optimal coherent control pulses (repeated π pulses at the antinodes of the oscillating Hamiltonian) designed to acquire maximum frequency information. This results in the effective total Hamiltonian $H_{\rm eff}(t)$. The acquired phase is the time integral of this function. (c) The frequency sensitivity is determined by varying ω, and a linear fit determines $d\phi/d\omega$. (d) The phase uncertainty $\delta\phi$ versus experimental repetition number N shows that the phase uncertainty is given by the binomial error $1/\sqrt{4N}$ (solid line). (e) The frequency sensitivity for the uncontrolled (red circles) and optimal control (blue diamonds) attains the respective limits (solid lines) for times shorter than the decoherence time. The error bars indicate the estimated standard deviation of slope $d\omega/d\phi$ from the linear regression fit as in panel (c). (e) (Inset) The quantum Fisher information associated with a given measurement protocol (uncontrolled, red; controlled, blue), determined from the slope of the acquired phase versus frequency is displayed on a log-log plot versus the time.

and yields better sensitivity over the no-control case as long as $\omega T > \pi$. This corresponds to a T^4 scaling of the QFI. At long times, decoherence of the qubit causes the QFI to decrease due to the increasing overlap of the states $|\psi_\omega\rangle$ and $|\psi_{\omega+d\omega}\rangle$.

The optimal Hamiltonian control yields a T^2 improvement over the QFI obtained with a standard Ramsey measurement. Given a finite time resource in metrology, such as the finite T_2^* time of the qubit, this yields a substantial improvement in QFI, amounting to a factor of 740 in this experimental demonstration.

In contrast to recent work [23,24], where T^3 scaling of the QFI has been observed for times limited only by the stability of an external reference, the T^4 scaling observed here is limited to times $T < T_2^*$. If we consider sensing for a duration longer than T_2, the optimal approach is to utilize repeated, back-to-back measurements each with duration T_2. By taking advantage of the fact that these repeated measurements sample the signal at different times, a T^3 scaling of the QFI for the total signal sampling time is also possible with our approach but with an optimized prefactor.

Having demonstrated such a significant improvement in the scaling of the quantum Fisher information with time, it is worth inquiring as to whether other Hamiltonian parameters can be estimated with such precision. For example, could the QFI associated with the amplitude $I_A^{(Q)}$ of the time-dependent Hamiltonian also achieve such scaling or at least an improvement under optimal control compared to the uncontrolled case? To address this, we again consider the eigenvalues of h_A, $\mu_\pm = \pm\sin(\omega t)/2$, which do not increase in time. As is well known from work with nitrogen-vacancy spin sensing [31–35], in this case the optimal control strategy is again to apply π rotations, but this time at *nodes* of the Hamiltonian, and yields an overall T^2 scaling of the quantum Fisher information as we discuss in Supplemental Material [36]. This is an improvement over the no-control case, where the maximum quantum Fisher information does not increase for longer interaction times.

We note that the optimal control needed to obtain the enhanced precision of the frequency depends on knowledge of the phase and frequency, which is itself the parameter to be estimated. Therefore, in general, we must apply adaptive control [37–40] where first some crude knowledge of the parameter is obtained without control, which is then used in the control Hamiltonian to obtain a more precise estimate of the parameter, which is fed back to adjust the coherent control in an adaptive loop until the optimal arrangement is converged upon. One might worry that the T^4 scaling is so sensitive to the matching of the time-dependent Hamiltonian and control that the T^4 scaling is difficult to achieve in practice. The degradation of the QFI due to frequency mismatch between the control and the parameter was analyzed for the case of a rotating magnetic field in Ref. [22], and, by applying a similar analysis here, we find that the QFI in the presence of a frequency mismatch $\Delta\omega$ is

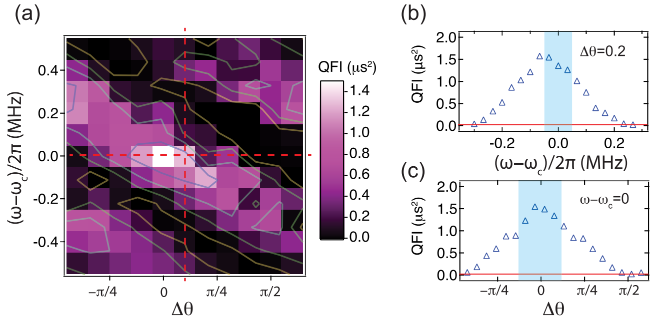

FIG. 3. Optimal control landscape. (a) Color plot of the QFI as two control parameters are swept for $T = 1.25$ μs: the phase difference between the control π pulses and the periodic Hamiltonian modulation (x axis) and the duration T_d between the π pulses (y axis) as specified by the control frequency $\omega_c = 2\pi/T_d$. The phase difference has been shifted slightly to account for a 6-ns delay between the control pulses and the periodic Hamiltonian. (b),(c) Line cuts through the control landscape [locations indicated as dashed red lines in (a)] show that for small parameter mismatches the QFI is still significantly greater than the uncontrolled case (red line). The blue regions show the parameter uncertainty based on an uncontrolled estimation using $N = 100$ experimental repetitions.

to leading order $I_\omega^{(Q)} = A^2T^4/\pi^2(1 - \Delta\omega^2T^2/2)$. Because the correction grows as T^2, an iterative procedure is required to refine the control frequency. The requirements on matching the phase of the control leads to a correction to the QFI proportional to $(1 - \Delta\theta^2)$, which depends only on the phase mismatch $\Delta\theta$ and does not grow with time [36]. In Fig. 3, we show the experimentally obtained quantum Fisher information for different mismatches between the phase and frequency of the control Hamiltonian. As shown in Fig. 3(a), the QFI reaches a maximum when the control is matched to the modulation frequency ω with a vanishing phase offset. Figure 3(a) also highlights how this control landscape can be mapped without a knowledge of the parameters that are to be estimated.

Figures 3(b) and 3(c) display the QFI versus the frequency and phase mismatch in detail. For the 1.25 μs interaction time considered here, the uncontrolled frequency and phase estimation based on $N = 100$ experimental repetitions (used to reduce the phase uncertainty) is sufficient to find the maximum in the QFI available with optimal control. Therefore, the robustness of the optimal control improvement in QFI to variations in the control parameters is sufficient to allow adaptive control to rapidly converge to the optimal values. In fact, in Ref. [22], it was proved that the number of iterations required to approach the maximum sensitivity grows only as a double logarithm of the total time T, and, in Supplemental Material [36], we discuss how an iterative procedure can be used to adaptively improve the frequency precision.

In quantum enhanced metrology, one seeks to take advantage of quantum properties to maximally utilize the available measurement resources. For parallel resources, such as the number of quantum systems, entanglement can be utilized to achieve Heisenberg scaling. We have demonstrated how quantum coherence, optimally harnessed through coherent control, can maximally utilize the serial resource: time. It is theoretically possible to combine both the serial and parallel resources which would give the best case quantum precision. The advantages conferred in frequency metrology with time-dependent Hamiltonians opens new horizons in precision measurement and time keeping.

We acknowledge P. M. Harrington, D. Tan, and J. T. Monroe for discussions, sample fabrication, and contributions to the experimental setup. We acknowledge research support from National Science Foundation (NSF) Grants No. DMR-1506081 and No. PHY-1607156, the Office of Naval Research (ONR) No. 12114811, and the Army Research Office (ARO) No. W911NF-15-1-0496. This research used facilities at the Institute of Materials Science and Engineering at Washington University. K. W. M. acknowledges support from the Sloan Foundation.

*murch@physics.wustl.edu

[1] S. Abe *et al.* (KamLAND Collaboration), Phys. Rev. Lett. **100**, 221803 (2008).
[2] B. Walker, B. Sheehy, L. F. DiMauro, P. Agostini, K. J. Schafer, and K. C. Kulander, Phys. Rev. Lett. **73**, 1227 (1994).
[3] M. Aguilar *et al.* (AMS Collaboration), Phys. Rev. Lett. **110**, 141102 (2013).
[4] G. Rosi, F. Sorrentino, L. Cacciapuoti, M. Prevedelli, and G. Tino, Nature (London) **510**, 518 (2014).
[5] L. Essen and J. Parry, Nature (London) **176**, 280 (1955).
[6] H. Lyons, Sci. Am. **196**, 71 (1957).
[7] A. D. Ludlow, M. M. Boyd, J. Ye, E. Peik, and P. O. Schmidt, Rev. Mod. Phys. **87**, 637 (2015).
[8] D. Gabor, J. Inst. Electr. Eng., Part 3 **93**, 429 (1946).
[9] H. Cramér, *Mathematical Methods of Statistics* (Princeton University, Princeton, NJ, 1946).
[10] R. A. Fisher, Math. Proc. Cambridge Philos. Soc. **22**, 700 (1925).
[11] S. L. Braunstein and C. M. Caves, Phys. Rev. Lett. **72**, 3439 (1994).
[12] S. L. Braunstein, C. M. Caves, and G. Milburn, Ann. Phys. (N.Y.) **247**, 135 (1996).
[13] S. Alipour, M. Mehboudi, and A. T. Rezakhani, Phys. Rev. Lett. **112**, 120405 (2014).
[14] M. Tsang, H. M. Wiseman, and C. M. Caves, Phys. Rev. Lett. **106**, 090401 (2011).
[15] V. Giovannetti, S. Lloyd, and L. Maccone, Science **306**, 1330 (2004).
[16] M. I. Kolobov, Rev. Mod. Phys. **71**, 1539 (1999).
[17] The LIGO Scientific Collaboration, Nat. Phys. **7**, 962 (2011).
[18] R. J. Sewell, M. Koschorreck, M. Napolitano, B. Dubost, N. Behbood, and M. W. Mitchell, Phys. Rev. Lett. **109**, 253605 (2012).
[19] W. M. Itano, J. C. Bergquist, J. J. Bollinger, J. M. Gilligan, D. J. Heinzen, F. L. Moore, M. G. Raizen, and D. J. Wineland, Phys. Rev. A **47**, 3554 (1993).
[20] V. Giovannetti, S. Lloyd, and L. Maccone, Phys. Rev. Lett. **96**, 010401 (2006).
[21] L. de Clercq, R. Oswald, C. Flühmann, B. Keitch, D. Kienzler, H.-Y. Lo, M. Marinelli, D. Nadlinger, V. Negnevitsky, and J. Home, Nat. Commun. **7**, 11218 (2016).
[22] S. Pang and A. N. Jordan, Nat. Commun. **8**, 14695 (2017).
[23] J. M. Boss, K. S. Cujia, J. Zopes, and C. L. Degen, Science **356**, 837 (2017).
[24] S. Schmitt *et al.*, Science **356**, 832 (2017).
[25] A. N. Jordan, Science **356**, 802 (2017).
[26] J. Yang, S. Pang, and A. N. Jordan, Phys. Rev. A **96**, 020301 (2017).
[27] T. Gefen, F. Jelezko, and A. Retzker, Phys. Rev. A **96**, 032310 (2017).
[28] J. Koch, T. M. Yu, J. Gambetta, A. A. Houck, D. I. Schuster, J. Majer, A. Blais, M. H. Devoret, S. M. Girvin, and R. J. Schoelkopf, Phys. Rev. A **76**, 042319 (2007).
[29] H. Paik *et al.*, Phys. Rev. Lett. **107**, 240501 (2011).
[30] D. Bures, Trans. Am. Math. Soc. **135**, 199 (1969).
[31] G. de Lange, D. Ristè, V. V. Dobrovitski, and R. Hanson, Phys. Rev. Lett. **106**, 080802 (2011).
[32] H. J. Mamin, M. Kim, M. H. Sherwood, C. T. Rettner, K. Ohno, D. D. Awschalom, and D. Rugar, Science **339**, 557 (2013).
[33] M. Loretz, S. Pezzagna, J. Meijer, and C. L. Degen, Appl. Phys. Lett. **104**, 033102 (2014).
[34] A. O. Sushkov, I. Lovchinsky, N. Chisholm, R. L. Walsworth, H. Park, and M. D. Lukin, Phys. Rev. Lett. **113**, 197601 (2014).
[35] I. Lovchinsky *et al.*, Science **351**, 836 (2016).
[36] See Supplemental Material at http://link.aps.org/supplemental/10.1103/PhysRevLett.119.180801 for further information about the sample parameters, amplitude estimation, iterative scaling, a comparison to Rabi spectroscopy, and statistical information are available in the Supplemental Material.
[37] G. Waldherr, J. Beck, P. Neumann, R. S. Said, M. Nitsche, M. L. Markham, D. J. Twitchen, J. Twamley, F. Jelezko, and J. Wrachtrup, Nat. Nanotechnol. **7**, 105 (2012).
[38] T. Baumgratz and A. Datta, Phys. Rev. Lett. **116**, 030801 (2016).
[39] H. Yuan and C.-H. Fred Fung, Phys. Rev. Lett. **115**, 110401 (2015).
[40] H. Yuan, Phys. Rev. Lett. **117**, 160801 (2016).